J|A|C|S
COMMUNICATIONS

Published on Web 10/20/2005

Gold-Caged Metal Clusters with Large HOMO−LUMO Gap and High Electron Affinity

Yi Gao, Satya Bulusu, and Xiao Cheng Zeng*

Department of Chemistry, University of Nebraska—Lincoln, Lincoln, Nebraska 68588

Received August 8, 2005; E-mail: xczeng@phase2.unl.edu

It has been known that certain magic metal clusters can mimic chemistry of halogen elements (e.g., the icosahedral cluster Al_{13}, coined as "superhalogen"),[1] aromatic molecules (e.g., square planar cluster Al_4^{2-}),[2] or nonmetal anionic component in salts (e.g., icosahedron cluster Tl_{13}^{11-} in a metallic Zintl phase).[3] In particular, highly stable clusters with large energy gap (>1.5 eV) between the highest occupied molecular orbital (HOMO) and lowest unoccupied molecular orbital (LUMO) may be perceived as a "superatom", analogous to fullerene C_{60} (with a large HOMO−LUMO gap $\Delta = 1.57$ eV)[4] that tends to retain its structure integrity and chemical identity in cluster-assembled solids.

Recently, a few highly stable (magic) gold-caged metal clusters with large HOMO−LUMO gaps have been reported in the literature. For example, the closed-shell icosahedral cluster $W@Au_{12}$ was predicted by Pyykkö and Runeberg[5] to have a large HOMO−LUMO gap, based on the density functional theory (DFT) calculation. Later, experiments by Li et al. confirmed the existence of the $W@Au_{12}$ icosahedral cluster, which has a measured HOMO−LUMO gap $\Delta = 1.68$ eV.[6] This energy gap is probably only second to that of the tetrahedral Au_{20} cluster, which has a measured gap $\Delta = 1.77$ eV.[4] To our knowledge, the tetrahedral Au_{20} cluster perhaps holds the record of having the largest HOMO−LUMO gap among medium-sized 3D metal clusters. Note that for neutral Au clusters, Gordon and co-workers recently showed that the 2D-to-3D transition may occur at Au_8.[7]

In this communication, we report a new series of isoelectronic gold-caged metal clusters, $M@Au_{14}$ (M = Zr, Hf), and anion clusters, $M@Au_{14}^-$ (M = Sc, Y). DFT calculations show that these gold-caged metal clusters have HOMO−LUMO gaps not only greater than the icosahedral gold-caged metal cluster $W@Au_{12}$ but even appreciably larger than the tetrahedral cluster Au_{20}. Moreover, the DFT calculations show that the neutral clusters $M@Au_{14}$ (M = Sc, Y) exhibit an electron affinity (EA) not only higher than the EA of "superhalogen" Al_{13} but also even higher than a Cl atom which has the highest elemental EA (3.61 eV).

We first performed an unbiased search for the global minimum structure of the $ZrAu_{14}$ mixed cluster, using the basin-hopping global optimization technique coupled with DFT method.[8] Four randomly constructed initial isomer structures (wherein three isomers having the Zr located at the outer shell) were used and all end up to the lowest-energy isomer (Figure 1 and Table S1) after a few tens of basin-hopping moves. Low-lying isomers were reoptimized using the BP86 functional[9] with the effective core potential (ECP) of the LANL2DZ basis set (see Figure S1).[10] Similar calculations were carried for other isoelectronic clusters $Hf@Au_{14}$ and $M@Au_{14}^-$ (M = Sc, Y) (Tables S2−S4). Next, harmonic vibrational frequencies were calculated to affirm that the lowest-energy isomer does not show imaginary frequencies (Tables S5 and S6). Finally, to examine basis set and functional effects on the predicted lowest-energy structures and their HOMO−LUMO gaps, the $Zr@Au_{14}$ and $Sc@Au_{14}^-$ were further optimized using both BP86 and PBE[11] functionals, along with a larger Stuttgart/Dresden (SDD) ECP valence basis[12] augmented by two sets of *f* functions (exponents = 1.425, 0.468) for Au. All calculations were performed using the Gaussian03 program.[13] The lowest-energy clusters $Zr@Au_{14}$ and $Hf@Au_{14}$ exhibit similar geometries: 14 outer gold atoms form a hollow cage with D_{2d} symmetry, while the Zr and Hf atom is enclosed in the gold cage. The four valence electrons of Zr (or Hf) plus the 14 valence s electrons of Au_{14} result in a total of 18 electrons, which is consistent with the 18-electron closed-shell rule.[5,6,14] Further DFT calculation confirms that $Zr@Au_{14}$ and $Hf@Au_{14}$ are all closed-shell structures (Table 1), similar to the icosahedral $W@Au_{12}$. However, there are still some notable structural differences between $M@Au_{14}$ and $W@Au_{12}$. In particular, the Au_{14} cage has eight rhombuses and eight triangles (Figure 1). The existence of a large number of rhombuses as a main structural feature has been rarely seen in low-lying gold-cage clusters. In all previously reported lowest-energy or low-lying gold-caged clusters, such as the gold fullerene Au_{32},[15] Au_{42},[16] or $W@Au_{12}$,[5,6] the gold atoms form raft triangles exclusively on the cage.

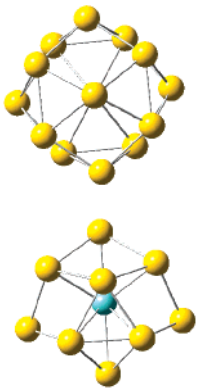

Figure 1. The top view (top) and side view (below) of the calculated D_{2d} $Zr@Au_{14}$ using the PBEPBE/SDD+Au(2f) functional and basis set. The Au−Au bond lengths vary between 2.713 and 2.84 Å.

In Table 1, we list the calculated bond lengths, HOMO−LUMO gaps, and frontier orbital configurations. For the Au_{14} cage, the peripheral Au−Au bond length varies between 2.713 and 2.840 Å, which is slightly shorter than the Au−Au bond length calculated by using the local-density approximation (2.89 Å) or generalized gradient approximation (2.97 Å).[17] In Table 1, we also list the calculated peripheral Au−Au bond length of $W@Au_{12}$ and Au_{20}, using the same functionals and basis set. It is worthy to note that the longest peripheral Au−Au bond length (2.83 Å) of $Zr@Au_{14}$ is less than the peripheral Au−Au bond length (2.894 Å) of $W@Au_{12}$, a manifestation of slightly stronger relativistic effects[5,18] in the Au_{14} cage.

Remarkably, as shown in Table 1 (boldfaced number), the calculated HOMO−LUMO gaps of the $W@Au_{12}$ and Au_{20} clusters are in good agreement with the experiments. These HOMO−LUMO

10.1021/ja055407o CCC: $30.25

Table 1. Calculated Properties of $Zr@Au_{14}$ and $Sc@Au_{14}^-$ versus $W@Au_{12}$, Au_{20}, and Al_{13}^- (experimental results in parentheses)

property	$Zr@Au_{14}$[a]	$Sc@Au_{14}^-$[a]	$W@Au_{12}$[a]	Au_{20}[a]	Al_{13}^-[b]
symmetry point group	D_{2d}	D_{2d}	I_h	T_d	I_h
HOMO−LUMO gap (eV)	**2.23/2.23**	2.04/1.99	**1.80/1.82 (1.68)**[c]	**1.85/1.82 (1.77)**[d]	1.85/1.90 (1.4)[e]
Frontier orbital configuration	$(b_1)^2(e)^4(a_1)^2(b_2)^0$	$(b_1)^2(a_1)^2(e)^4(a_1)^0$	$(t_{1u})^6(t_{2g})^6(h_g)^{10}(h_g)^0$	$(t_1)^6(t_2)^6(e)^4(t_2)^0$	$(t_{2u})^6(t_{1u})^6(g_u)^8(h_g)^0$
HOMO (eV)	−5.81/−5.65	−2.49/−2.34	−5.53/−5.39	−5.87/−5.71	−1.94/−1.91
Au−Au bond length (Å)					
shortest	2.719/2.713	2.719/2.715	2.894/2.890	2.679/2.679	
longest	2.830/2.840	2.827/2.835		2.830/2.827	
M-Au bond length (Å)					
shortest	2.822/2.803	2.763/2.745	2.752/2.749		
longest	2.923/2.922	2.900/2.901			
EA (eV)		**4.13/3.97**[f]			**3.38/3.35 (3.57)**[g]

[a] BP86/PBE (SDD+Au(2f)). [b] BP86/PBE (6-31G*). [c] Reference 6. [d] Reference 4. [e] Reference 1c. [f] BP86/PBE (LANL2DZ). [g] Reference 1d.

gap results suggest that the BP86 functional along with the ECP of SDD+Au(2f) (or even the smaller LANL2DZ) basis set is quite reliable in predicting energy gaps of gold clusters (for both clusters, the error bar is less than 0.2 eV), particularly in predicting the relative difference in the HOMO−LUMO gap between two gold clusters, for which the error bar appears to be even smaller than 0.2 eV.

Also shown in Table 1 and Table S6, the calculated HOMO−LUMO gaps of $Zr@Au_{14}$ and $Hf@Au_{14}$ are $\Delta \sim 2.23$ and 2.05 eV, respectively. These values are appreciably larger than the calculated HOMO−LUMO gaps $\Delta \sim 1.8$ eV for $W@Au_{12}$ and $\Delta \sim 1.85$ eV for Au_{20}. Because the HOMO−LUMO gap difference between $Zr@Au_{14}$ and Au_{20} amounts to 0.38 eV, the measured HOMO−LUMO gap of $Zr@Au_{14}$ is also likely larger than the measured gap ($\Delta \sim 1.77$ eV) of Au_{20}. Assuming the HOMO−LUMO gap difference between $W@Au_{12}$ and Au_{20} can be a guide, we expect that the measured gap of $Zr@Au_{14}$ may be even close to 2 eV. In addition to the 18-electron rule, two other reasons for the high stability and large HOMO−LUMO gap of the $Zr@Au_{14}$ are due to the relativistic effects and aurophilic attraction.[5,18] These two effects can be seen from a direct comparison of high-frequency modes, core−shell binding energy (Table S7), and HOMO−LUMO gap of $Zr@Ag_{14}$ versus $Zr@Au_{14}$ (Table S5). Indeed, most force constants for the high-frequency modes are larger for Au than Ag, due to the relativistic increase of the stretching force constants.

As noted in the above, the neutral Al_{13} cluster behaves like a superhalogen because of its high EA value, which is very close to the EA of a Br atom (Table S8). In Table 1, we also show the calculated EA values (∼3.38 eV) and the measured one (3.57 eV) of the icosahedral Al_{13}^- cluster,[1d] which are in good agreement with each other. As shown in Table 1 and Table S8, since the calculated EA and vertical detachment energy (VDE) values of $M@Au_{14}^-$ (M = Sc, Y) are 0.5−0.75 eV higher than the calculated EA and VDE values of Al_{13}^-, it is very likely that the measured EA and VDE of $M@Au_{14}^-$ (M = Sc, Y) are greater than those of Al_{13}^-, as well. As such, the neutral clusters $M@Au_{14}$ (M = Sc, Y) are expected to have an EA not only higher than the superhalogen Al_{13}, but possibly even higher than a Cl atom, which has the highest (measured) elemental EA or VDE (3.61 eV; see Table S8).[19]

In summary, we present a new series of isoelectronic gold-caged metal clusters, $M@Au_{14}$ (M = Zr, Hf), and anion clusters, $M@Au_{14}^-$ (M = Sc, Y), all having a HOMO−LUMO gap larger than the $W@Au_{12}$ and Au_{20} clusters (both known with a large *measured* HOMO−LUMO gap >1.6 eV). Moreover, the neutral clusters $M@Au_{14}$ (M = Sc, Y) exhibit a calculated EA not only higher than the calculated EA of the superhalogen icosahedral Al_{13} cluster but also possibly even higher than a Cl atom, which has the highest (measured) elemental EA or VDE.

Acknowledgment. This work was supported by grants from NSF, DOE (DE-FG02-04ER46164), and the Nebraska Research Initiative, and by John Simon Guggenheim Foundation and the Research Computing Facility at University of Nebraska−Lincoln.

Supporting Information Available: Data of Cartesian coordinates, harmonic vibrational frequencies, relative energies, core−shell binding energies, VDE/EA, energy levels, and the complete ref 13 are collected. This material is available free of charge via the Internet at http://pubs.acs.org.

References

(1) (a) Gutsev, G. L.; Boldyrev, A. I. *Chem. Phys.* **1981**, *56*, 277−283. (b) Wang, X.-B.; Ding, C.-F.; Wang, L.-S.; Boldyrev, A. I.; Simons, J. *J. Chem. Phys.* **1999**, *110*, 4763−4771. (c) Bergeron, D. E.; Castleman, A. W.; Morisato, T.; Khanna, S. N. *Science* **2004**, *304*, 84−87. (d) Li, X.; Wang, L.-S. *Phys. Rev. B* **2000**, *65*, 153404.
(2) Li, X.; Kuznetsov, A. E.; Zhang, H.-F.; Boldyrev, A. I.; Wang, L.-S. *Science* **2001**, *291*, 859−861.
(3) Dong, Z. C.; Corbett, J. D. *J. Am. Chem. Soc.* **1995**, *117*, 6447−6455.
(4) Li, J.; Li, X.; Zhai, H.-J.; Wang, L.-S. *Science* **2003**, *299*, 864−867.
(5) Pyykkö, P.; Runeberg, N. *Angew. Chem., Int. Ed.* **2002**, *41*, 2174−2176.
(6) Li, X.; Kiran, B.; Li, J.; Zhai, H.-J.; Wang, L.-S. *Angew. Chem., Int. Ed.* **2002**, *41*, 4786−4789.
(7) Olson, R. M.; Varganov, S.; Gordon, M. S.; Metiu, H.; Chretien, S.; Piecuch, P.; Kowalski, K.; Kucharski, S. A.; Musial, M. *J. Am Chem. Soc.* **2005**, *127*, 1049.
(8) (a) Wales, D. J.; Scheraga, H. A. *Science* **1999**, *285*, 1368−1372. (b) Yoo, S.; Zeng, X. C. *Angew. Chem., Int. Ed.* **2005**, *44*, 1491−1494.
(9) (a) Becke, A. D. *Phys. Rev. A* **1988**, *38*, 3098−3100. (b) Perdew, J. P. *Phys. Rev. B* **1986**, *33*, 8822−8824.
(10) (a) Hay, P. J.; Wadt, W. R. *J. Chem. Phys.* **1985**, *82*, 270−283. (b) Wadt, W. R.; Hay, P. J. *J. Chem. Phys.* **1985**, *82*, 284−298. (c) Hay, P. J.; Wadt, W. R. *J. Chem. Phys.* **1985**, *82*, 299−310.
(11) Perdew, J. P.; Burke, K.; Ernzerhof, M. *Phys. Rev. Lett.* **1996**, *77*, 3865−3868.
(12) (a) Dolg, M.; Wedig, U.; Stoll, H.; Preuss, H. *J. Chem. Phys.* **1987**, *86*, 866−872. (b) Schwerdtfeger, P.; Dolg, M.; Schwarz, W. H. E.; Bowmaker, G. A.; Boyd, P. D. W. *J. Chem. Phys.* **1989**, *91*, 1762−1774.
(13) Frisch, M. J. et al. *Gaussian 03*, revision C.02; Gaussian, Inc.: Wallingford CT, 2004.
(14) Hirsch, A.; Chen, Z.; Jiao, H. *Angew. Chem., Int. Ed.* **2000**, *39*, 3915−3917.
(15) Johansson, M. P.; Sundholm, D.; Vaara, J. *Angew. Chem., Int. Ed.* **2004**, *43*, 2678−2681.
(16) Gao, Y.; Zeng, X. C. *J. Am. Chem. Soc.* **2005**, *127*, 3698−3699.
(17) Häberlen, O. D.; Chung, S.-C.; Stener, M.; Rösch, N. *J. Chem. Phys.* **1997**, *106*, 5189−5201.
(18) Pyykkö, P. *Angew. Chem., Int. Ed.* **2002**, *41*, 3573.
(19) Lide, D. R. *CRC Handbook of Chemistry and Physics*, 73rd ed.; CRC Press: Boca Raton, FL, 1992.

JA055407O